Preparation and characterization of fluoride conversion coating on biodegradable AZ31B magnesium alloy

TINGTING YAN[a,b,*], LILI TAN[b], BINGCHUN ZHANG[b], KE YANG[b]
[a]Faculty of Materials Science and Engineering, Kunming University of Science and Technology, Kunming, 650093, China
[b]Institute of Metal Research, Chinese Academy of Sciences, Shenyang, 110016, China

A compact fluoride conversion coating was prepared on AZ31B magnesium alloy by reaction with hydrofluoric acid. Morphology, composition and corrosion resistance of the coating were studied. The SEM examination showed that a compact film with some irregular distributed pores was formed on the surface of sample. The XPS analysis indicated that the coating was mainly composed of MgO and MgF_2. Potentiodynamic polarization indicated that the fluoride conversion coating resulted in higher corrosion potential, lower corrosion current density, and a significant enhancement in corrosion resistance of AZ31B. The phosphate-calcium coating formed on the surface of fluoride treated AZ31B indicated a good bioactivity of the material.

1. Introduction

Magnesium (Mg) and its alloys are being employed as potential implant materials due to their outstanding mechanical properties and unique biological characteristics. For example, the Young's modulus of pure magnesium is about 45 GPa [1], which is more close to that of human bone (17.0-18.9) GPa in comparison to other metallic materials like Ti-alloys, Co-Cr alloys or stainless steel [2]. At the same time a better match in elastic modulus drastically reduces the stress shielding effects that exist in current metallic implants of stainless steel or titanium alloys due to their higher elastic modulus than the natural bone and a reduced stimulation of new bone growth [3]. Large amount of Mg ions exist in human body and these are involved in almost all the metabolic reactions [4]. The daily intake of Mg ions for an adult has been shown to be about 2.2-6.3 mmol and the redundant Mg^{2+} can be harmlessly excreted in the urine [5]. Therefore, the low corrosion resistance property, the main drawback of Mg in many engineering application, makes it suitable for use as a potential biodegradable implant material. However, the problems associated with Mg and its alloys, such as alkalization, hydrogen release and high concentration of Mg ions [6,7], resulting from high corrosion rate of magnesium, limit their clinical applications.

Currently, the key issue in the development of biodegradable Mg implants is to slow down the corrosion rate of these alloys to reasonably low values [8-10]. One of the effective methods to reduce the corrosion rate of Mg and its alloys is the surface treatment, which is also beneficial in improving the bioactivity of biomaterials. Hence, it is possible to improve the surface bioactivity and corrosion resistance of Mg alloy by a proper surface treatment. A number of coating techniques such as Ca-P coating [11], micro-arc oxidized calcium phosphate coating [12], calcium phosphate glass coating [13], calcium phosphate conversion coating [14], nano-HA/MgF_2 -DCPD/MgF_2 composite coating [15] have been developed to reduce the corrosion of Mg alloys. These have been shown to improve the surface bioactivity and corrosion resistance of Mg alloy to different extent. These findings have given the much needed boost to the confidence of the researcher in regard to the use of Mg implants. However, there is still enough space for the development of more coating techniques that are able to meet the stringent requirements of implants.

Fluoride is the essential element of diet and is required for normal dental and skeletal growth [16]. It is also one of the few known agents that can stimulate osteoblast proliferation and increase new mineral deposition in cancellous bone. The incorporation of fluoride into the bone increases the size and, thus, decreases the solubility of the bone apatite crystals [17]. Therapeutic future for sodium fluoride in osteoporosis lies with early administration and low-dose regimens in which toxic blood levels are avoided and mineralization is not impaired [18]. One of the studies carried out by Ellingsen et al. [19] revealed that the SR-NaF group could significantly reduce the risk of vertebral fractures and results in increased spinal bone mass without reducing bone mass at the femoral neck and total hip. An

experimental study in dogs revealed that the fluoride modified implant surface promotes osteointegration in the early phase of healing following implant installation[20]. An evaluation of available literature shows that the fluoride has been used clinically for the prevention and treatment of osteoporosis although controversies still exist.

In light of the above statements, a fluoride conversion coating was prepared on the surface of AZ31B Mg alloy. The morphology, composition and corrosion resistance of this coating were studied.

2. Experimental

2.1 Sample preparation and fluoride conversion treatment

The test material used for the study was a conventional AZ31B extruded Mg alloy, with a composition of 1.2 % Al, 0.74 % Zn, 0.35 % Mn, 0.026 % Si, 0.003 % Fe, 0.0028 % Cu, 0.0003 % Ni (wt %) and balance Mg. The ingot was cut into plates of size 11 mm×11 mm×3 mm, mechanically polished up to 2,000 grit with SiC paper and then ultrasonically rinsed with acetone, absolute ethanol and distilled water, successively. For conversion treatment, the specimens were immersed in a plastic bottle containing HF of different concentrations ranging from 30 % to 50 % (wt %)) at 30 °C for different times from 12 h to 48 h. Three different experimental parameters were selected for comparison. They are 30 % HF-48 h, 50 % HF-12 h and 50 % HF-48 h. The treated specimens were rinsed with distilled water and dried in an oven at 40 °C.

2.2 Characterization

The morphology of the surface layer was examined by scanning electron microscope (SEM, JEOL JSM-6301F). The composition of the layer was analyzed by X-ray photoelectron spectroscopy (XPS, Thermo VG ESCALAB250).

2.3 Electrochemical test

Electrochemical polarization experiments were carried out using a potentiostat/galvanostat model 237A corrosion measurement system. Polarization measurements were carried out in simulated blood plasma containing NaCl 6.8 g/L, $MgSO_4$ 0.1 g/L, $NaHCO_3$ 2.2 g/L, Na_2HPO_4 0.216 g/L, NaH_2PO_4 0.026 g/L, $CaCl_2$ 0.2 g/L, KCl 0.4 g/L, at a temperature of 37 °C. The area of specimen, exposed to the solution was 1cm^2. The scans were started at the corrosion potential in the anodic or cathodic directions with the scanning rate of 0.5 mV/s. A three-electrode cell consisting of the specimen as the working electrode, the saturated calomel electrode as reference and the platinum as counterelectrode were used for the measurements.

2.4 Immersion test

Immersion test was conducted in simulated blood plasma. The pH value of the solution was adjusted to 7.4. The specimens with different treatments were immersed vertically in an airtight container containing such solution. The ratio of the specimen area to the solution volume was taken as 3 cm^2/mL, according to ISO 10993-12 [21]. Specimens without any surface treatment (labeled as untreated) were used as controls. All the immersion containers were kept at 37 °C in a 5 % CO_2 incubator. The immersion solution was changed every day. The pH values of the solution were measured by PHS-2C acidometer at different times. The surface appearance of samples with corrosion products was observed by SEM, and the composition of the corrosion products after immersion for 120 days was analyzed by energy dispersive spectrometry (EDS, Oxford INCA Energy 300).

3. Results

3.1 Microstructure of conversion coating

Fig. 1 shows the surface morphology of the conversion coating on AZ31B. It is seen that a compact film is developed successfully on the surface of AZ31B sample. Some irregular pores scattered in the coating could also be observed. A good bonding appears to exist between a uniform film and the substrate, as illustrated in Fig. 2.
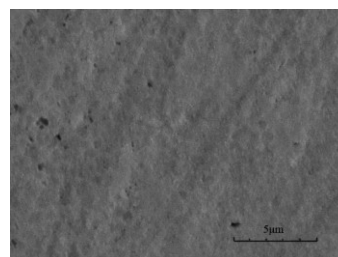

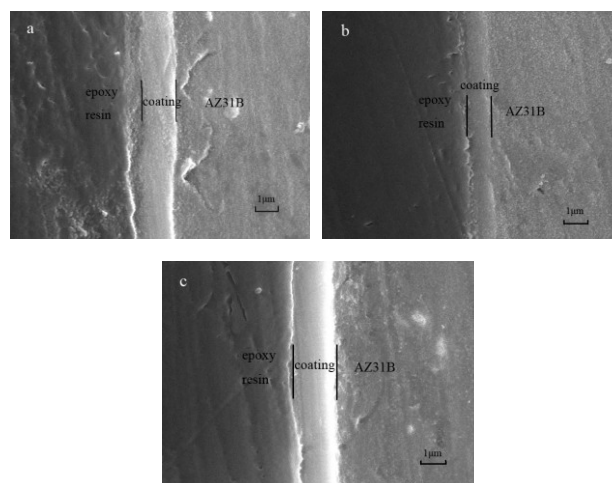*Fig. 1. SEM micrographs of conversion coating on AZ31B.*

Fig. 2. SEM micrographs of cross-section of fluoride treated AZ31B sample (a: 30 % HF-48h; b: 50 % HF-12 h; c: 50 % HF-48 h).

The coatings with different thicknesses were obtained by controlling process parameters. The thicknesses of coatings under conditions of 30 % HF-48h, 50 % HF-12 h and 50 % HF-48 h are about 1.7 μm, 1.0 μm and 1.9 μm, respectively, as shown in Fig. 2.

The XPS survey scan of the surface of fluoride-coated Mg is shown in Fig. 3. It is obvious that the conversion coating mainly consists of O, Mg, F elements. Fig. 4 shows Mg_{2p} XPS spectra for the treated AZ31B. From the binding energy, it can be concluded that Mg exists in the coating in the form of MgO and MgF_2. The results correlate well with the elemental composition listed in Table 1. The high concentration of carbon commonly seen on the surface in XPS surface scan may be due to the adventitious hydrocarbons from the environment.
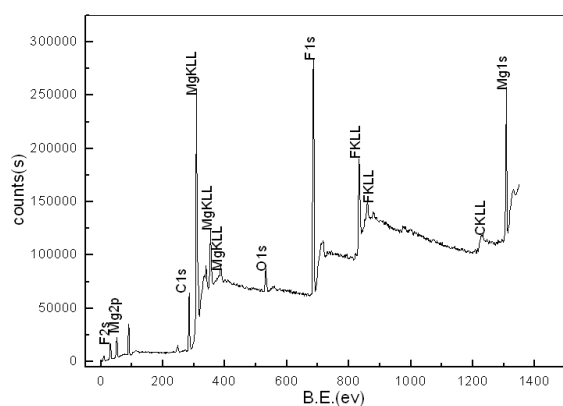

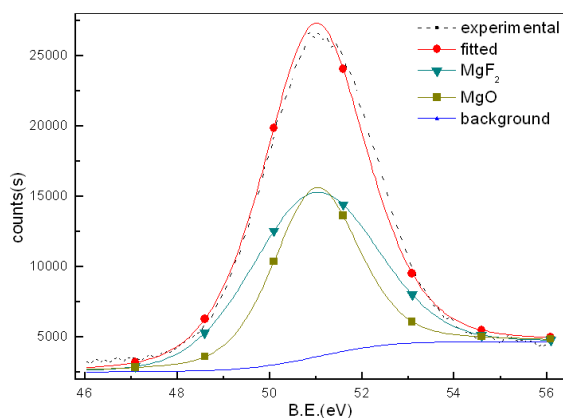Fig. 3. XPS spectra of fluoride treated AZ31B magnesium alloy.

Fig. 4. Fitting results for Mg_{2p} spectra for surface coating.

Table 1. Elemental composition of the conversion coating on AZ31B.

Elements	C	O	Mg	F
Atomic%	31.88	6.11	43.78	18.23

3.2 Electrochemical test

Fig. 5 shows the polarization curves of the treated and untreated AZ31B samples. The corrosion potential, E_{corr}, and the corrosion current density, I_{corr}, obtained from these curves are given in Table 2. A relatively higher corrosion potential is observed in the polarization curves of fluoride treated samples. The corrosion current density of treated samples is found to be about three orders of magnitude lower than that of untreated AZ31B samples. So it can be concluded that fluoride treated samples have a lower corrosion rate than untreated samples. Table 2 also reveals that the corrosion resistance ranks in the following order: untreated < 50 % HF 12 h treated < 30 % HF 48 h treated < 50 % HF 48 h treated, with the corrosion potential of -1.488 V, -1.453 V, -1.430 V, -1.429 V, respectively, and the corrosion current density of $(A \cdot cm^{-2})$ of 1.907×10^{-4}, 1.104×10^{-7}, 5.552×0^{-8} and 2.486×10^{-8}, respectively.

Table 2. Corrosion potentials and corrosion currents.

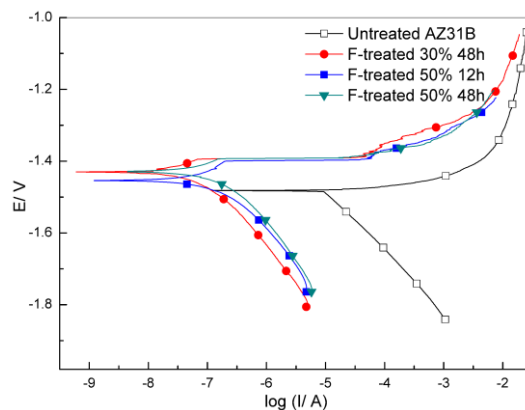| Samples	Corrosion Potential E_{corr} / (V)	Corrosion Current i_{corr} / (A·cm^{-2})
Untreated AZ31B	-1.488	1.907×10^{-4}
30%HF 48h treated	-1.430	5.552×10^{-8}
50%HF 12h treated	-1.453	1.104×10^{-7}
50%HF 48h treated	-1.429	2.486×10^{-8}

Fig. 5. Polarization curves of treated and untreated AZ31B.

3.3 Immersion test

The surface morphologies of the fluoride treated samples after immersion for different times in simulated blood plasma are shown in Fig. 6. After 5 days of immersion, white particles are deposited on the surface. After 20 days, a compact coating with some small cracks was formed on the surface as well as some white particles

sediment as that of 5 days immersion. After 60 days, the coating obviously was grown. On the 120-th day, a thicker coating composed of spherical crystals was found on the surface and some larger cracks than that of 20-day immersion form on the surface. The presence of cracks may possibly be attributed to desorption of water during drying process. The EDS analysis of the surface of AZ31 with fluoride conversion coating after 20 days immersion indicates that the corrosion product is a compound of phosphate and calcium, as shown in Fig. 7. The Ca/P ratio of the compound is about 1.57, close to that of hydroxyapatite (HA).
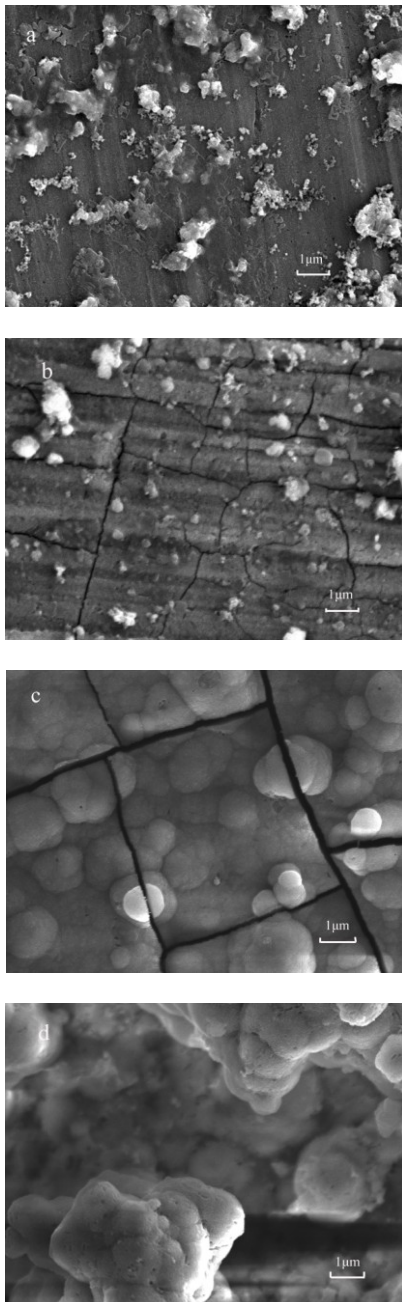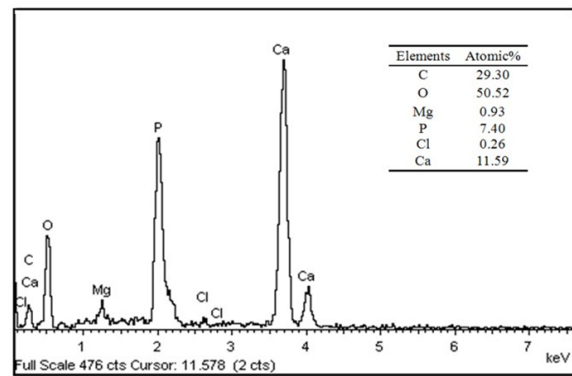

Fig. 7. EDS analysis of fluoride treated AZ31B incubating in simulated blood plasma for 120days.

Fig. 8 shows the pH value of simulated blood plasma incubating fluoride treated and untreated AZ31B samples. The lower pH value usually represents a higher corrosion resistance known from the corrosion principle of Mg. It can be concluded that: (1) Fluoride treated samples have higher corrosion resistance than untreated ones: the pH values of solution incubating treated samples are lower than that of untreated samples after 120 days of immersion. (2) The changing tendency of pH value of solution treated sample is slower than that of untreated one. The former keeps below 9.0 until the 30-th day, while the latter reached about 11.0 on the second day. (3) The specimens treated using long-time higher HF concentration has higher corrosion resistance and the result corresponds with that of the electrochemical test.
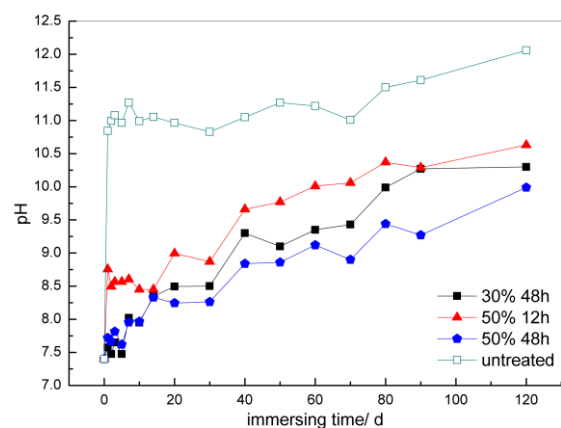

Fig. 6. Surface morphologiesof fluoride treated specimens incubating in simulated blood plasma for (a) 5days, (b) 20days, (c) 60days, (d) 120days.

Fig. 8. The pH value of simulated blood plasma incubating treated and untreated AZ31B samples as a function immersion time.

4. Discussion

From the aforementioned experimental results, it can be inferred that the coating of fluoride on AZ31B alloy can play an effective role in enhancing its corrosion resistance in simulated blood plasma resulting an improvement in blood-compatibility of this alloy.
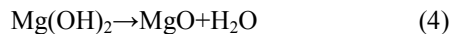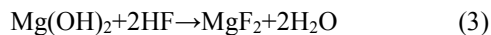
XPS results indicate that the coating is mainly composed of MgF_2 and MgO. MgF_2 is formed *via* a replacement reaction given below:

$$Mg+HF \rightarrow MgF_2+H_2\uparrow \qquad (1)$$
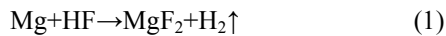
An oxidation reaction occurs as following:

$$Mg+2H_2O \rightarrow Mg(OH)_2+H_2\uparrow \qquad (2)$$
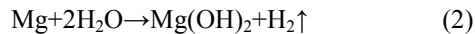
Since $Mg(OH)_2$ is not stable in acidic solution [22], reactions occur as following:

$$Mg(OH)_2+2HF \rightarrow MgF_2+2H_2O \qquad (3)$$

$$Mg(OH)_2 \rightarrow MgO+H_2O \qquad (4)$$

These reactions take place at the film-solution interface [23]. The perfect insoluble MgF_2 layer which acts as a passive film is formed on the Mg alloy surface by a chemical reaction.

The irregular pores in the film are generated due to the generation of hydrogen and may get decreased or filled by the precipitation of MgF_2 and MgO particles [23] during the treatment. MgF_2 film grows with immersion time, but the growth rate slows down as immersion continues [24]. The reaction rate between Mg alloy and HF increases with increasing concentration of HF. The higher concentration of HF has been shown to promote the growth of passive film [25], which is, to some extent beneficial in removing the pores resulting from hydrogen generation, significantly improving the corrosion resistance.

A biodegradable material has a controllable dissolution rate or a delayed corrosion process. Implanted medical devices made of such degradable material retain their mechanical and biological properties before the surgical region recovers or heals. After this initial period, it gradually gets dissolved or absorbed. The result of immersion test revealed that the treated specimen is corroded slightly in the initial stage and the rate of corrosion becomes fast with increasing time, which meets the demand of degradable implants. On the other hand, coating with fluoride film of varying thickness can be ideally adapted for different implantation places.

5. Conclusions

A compact fluoride conversion coating was successfully prepared on AZ31B Mg alloy. Different thickness of coatings could be prepared varying different experimental parameters. Microstructural features showed that the coating was mainly composed of MgF_2 and MgO. Electrochemical and immersion tests showed an improved corrosion resistance for the fluoride treated AZ31B alloy in simulated blood plasma compared with that of untreated

AZ31B alloy samples. It was revealed that the corrosion behavior of fluoride coated AZ31B sample meets the requirement of degradable implant material. Furthermore, the results showed that the corrosion resistance of the coatings is related to their thickness. Thus, coatings with fluoride film of varying thickness can be ideally adapted for different implantation places.

References

[1] J. Zhang, Z. H. Zhang, Magnesium alloys and their application (Chemical Industry Press, Beijing, 2004).
[2] F. Witte, N. Hort, C. Bogt, S. Cohen, K. U. Kainer, R. Willunmeit, F. Feyerabend, Curr. Opin. Solid St. M. **12**, 63 (2008).
[3] P. Mark, Staiger, M. Alexi, J. Huadmai, G. Dias, Biomater. **27**, 1728 (2006).
[4] A. Hruby, N. M. Mckeown, http://dx.doi.org/10.1016/B978-0-12-397153-1.00032-9.
[5] N. E. Saris, E. Mervaala, H. Karppanen, J. A. Khawaja, A. Lewenstam, Clin. Chim. Acta. **294**, 1 (2000).
[6] B. Ullmann, N. Angrisani, J. Reifenrath, J. M. Seitz, D. Bormann, F. W. Bach, A. M. Lindenberg, Mater. Sci. Eng. C **33**, 3010 (2013).
[7] G. L. Song, Adv. Eng. Mater. **7**, 563 (2005).
[8] F. Witte, V. Kaese, H. Haferkamp, A. M. Lindenberg, C. J. Wirth, H. Windhagen, Biomater. **26**, 3557 (2005).
[9] B. R. Sunil, A. A. Kumar, T. S. Kumar, U. Chakkingal, Mater. Sci. Eng. **33**, 1607 (2013).
[10] Y. M. Wang, J. W. Guo, Z. K. Shao, J. P. Zhuang, M. S. Jin, C. J. Wu, D. Q. Wei, Y. Zhou, Sur. Coat. Tech. **219**, 84 (2013).
[11] X. Xiao, H. Yu, Q. Zhu, G. Li, Y. Qu, R. Gu, Bionic Eng. **10**, 156 (2013).
[12] Y. K. Pan, C. Z. Chen, D. G. Wang, T. G. Zhao, Coll. Sur. **109**, 1 (2013).
[13] M. Ren, S. Cai, G. Xu, X. Ye, Y. Dou, K. Huang, X. Wang, Non-Crys. Soli. **269**, 69 (2013).
[14] L. P. Xu, F. Pan, G. N. Yu, E. L. Zhang, K. Yang, Biomater. **30**, 1512 (2009).
[15] H. R. Bakhsheshi, M. H. Idris, M. R. Kadir, Sur. Coat. Tech. **222**, 79 (2013).
[16] W. Mertz, Sci. **213**, 1332 (1981).
[17] C. Palmer, S. H. Wolfe, J. Am. Diet. Assoc. **105**, 1620 (2005).
[18] R. Balena, M. Kleerekoper, J. A. Foldes, M. S. Shih,

D. S. Rao, H. C. Schober, A. M. Parfitt, Osteoporosis Int. **9**, 428 (1998).

[19] J. E. Ellingsen, C. B. Hohansson, A. Wennerber, A. Holmén, Int. J. Oral Max. Impl. **19**, 659 (2004).

[20] T. Berglundh, I. Abrahamsson, J. P. Albouy, J. Lindhe, Clin. Oral. Impl. Res. **18**, 147 (2007).

[21] ISO 10993-12, Biological evaluation of medical devices-part 12: Sample preparation and reference materials, 2007.

[22] M. Pourbaix, J. Muylder, Atlas d'équilibres électrochimiques (Gauthier-Villars et Cie, Paris, 1963).

[23] S. Verdier, N. V. Laak, S. Delalande, J. Metson, F. Dalard, Appl. Surf. Sci. **235**, 513 (2004).

[24] K. Y. Chiu, M. H. Wang, F. T. Cheng, H. C. Man, Surf. Coat. Tech. **201**, 590 (2007).

[25] J. Z. Li, J. G. Huang, Y. W. Tian, C. S. Liu, Tran. Nonferrous Met. So. China **19**, 50 (2009).

_____
[*]Corresponding author: yantting@gmail.com